

## **Operation Mechanism of Organic Electrochemical Transistors as Redox Chemical Transducers**

Siew Ting Melissa Tan<sup>1</sup>, Scott Keene<sup>2</sup>, Alexander Giovannitti<sup>1</sup>, Armantas Melianas<sup>1</sup>, Maximilian Moser<sup>3</sup>, Iain McCulloch<sup>3,4</sup>, Alberto Salleo<sup>1\*</sup>

<sup>1</sup>Department of Materials Science and Engineering, Stanford University, California 94305, USA

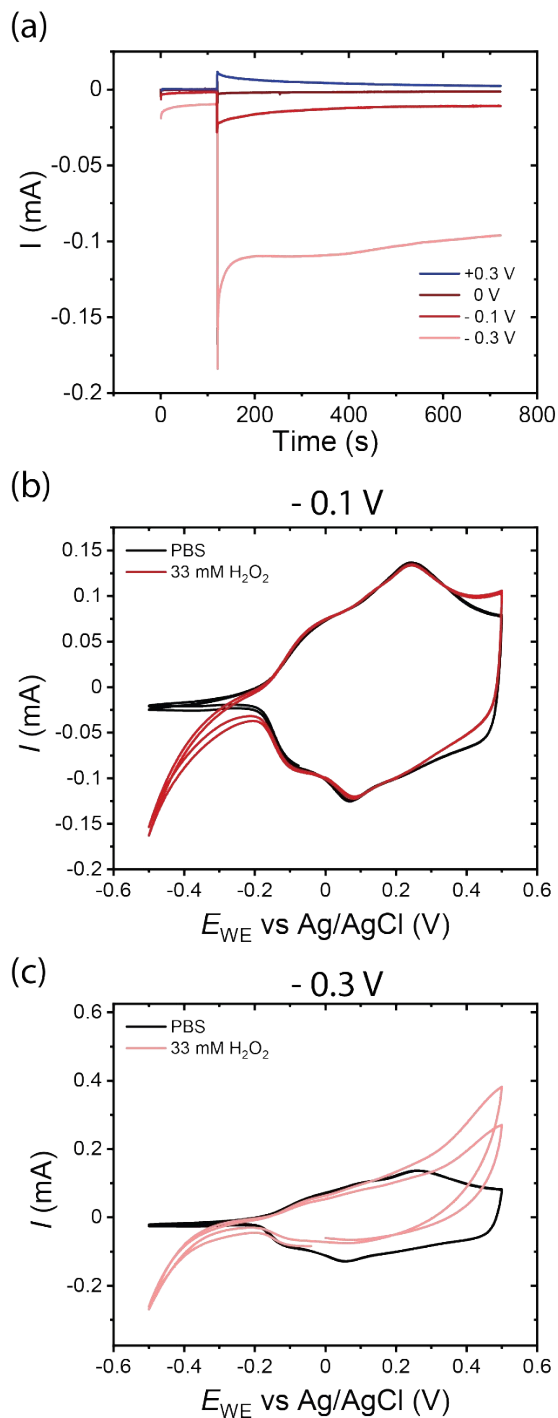
<sup>2</sup>Electrical Engineering Division, Department of Engineering, University of Cambridge, Cambridge, United Kingdom

<sup>3</sup>Department of Chemistry, Chemistry Research Laboratory, University of Oxford, Oxford, OX1 3TA, UK

<sup>4</sup>Physical Science and Engineering Division, King Abdullah University of Science and Technology, Thuwal 23955-6900, Saudi Arabia

\*Corresponding author email: [asalleo@stanford.edu](mailto:asalleo@stanford.edu)

## Supplementary Information



**SI Figure 1. Effect of different applied voltages on a p(g3T2) electrode exposed to  $H_2O_2$ .** (a) Chronoamperometric measurements of a spin coated film of p(g3T2) on ITO/glass held at voltages of + 0.3 V, 0 V, - 0.1 V and - 0.3 V vs. a saturated Ag/AgCl reference electrode. 33mM  $H_2O_2$  is added at 60 s. (b) Cyclic voltammetry of p(g3T2) film in its pristine state in PBS (black) and after

chronoamperometry at -0.1V and addition of H<sub>2</sub>O<sub>2</sub>. **(c)** Cyclic voltammetry of p(g3T2) film in its pristine state in PBS (black) and after chronoamperometry at -0.3V and addition of H<sub>2</sub>O<sub>2</sub>.

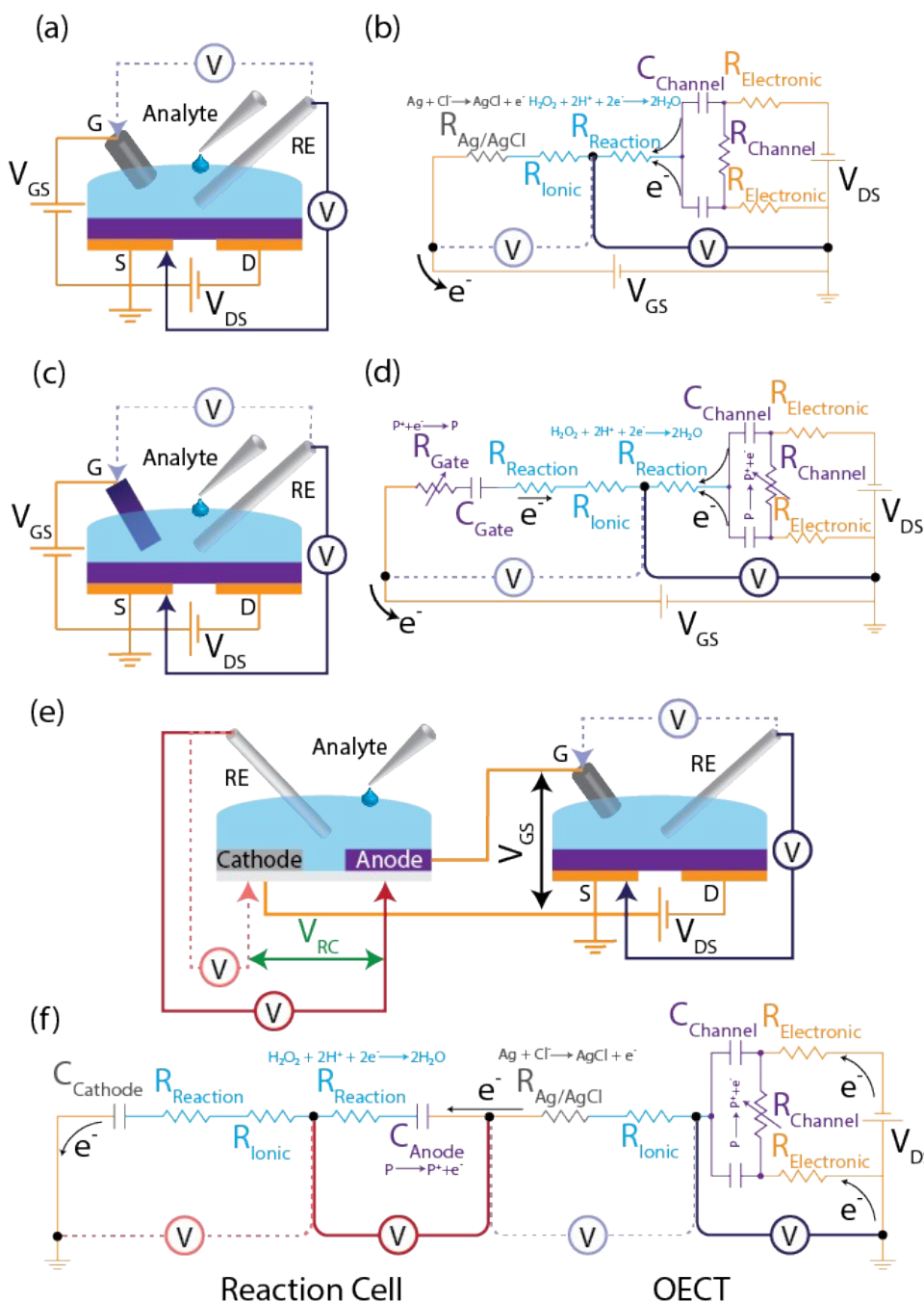
It is important to understand the effect of electrode potential on the rate of redox reactions (faradaic currents) for amperometric OECTs. Applying a gate voltage results in changes in channel potential which modulates the channel's ability to undergo redox reactions. Furthermore, the application of a drain voltage across the channel results in asymmetry in potentials across the channel.

To investigate the effect of electrode potentials on reaction currents, chronoamperometry was conducted on p(g3T2) electrodes in the presence of H<sub>2</sub>O<sub>2</sub>. Potentials are determined in related to a saturated Ag/AgCl reference electrode. Different working electrode potentials were applied while current was measured.

Different potentials applied on the working electrode changes the initial energy level of electrons in the OMIEC electrode (degree of filling of the HOMO). The more negative potentials applied on the electrode, the more reduced the OMIEC and the higher the energy of these electrons. Hence, the driving force for electron transfer from the OMIEC electrode to the redox analyte in the electrolyte increases with more negative applied potentials (**SI Figure 1 (a)**). Applying too extreme potentials also results in degradation of the material as seen by the change in the CV after imposing -0.3V (**SI Figure 1 (c)**).

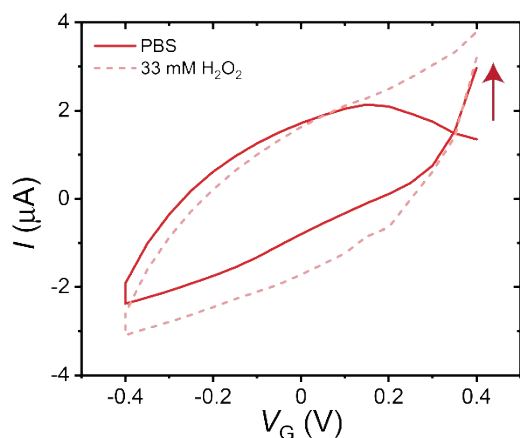
OECT drain voltages are usually on the order of 100 mV. In amperometric OECTs where redox analytes are added to the electrolyte, the potential differences across the channel can result in drastic differences in reaction rates. The difference in faradaic reaction current between 0 V and -0.1V is an order of magnitude (from 1 uA to 10 uA). Hence, applying a relatively small drain voltage of 100mV results in great differences in faradaic currents on the source versus the drain. Hence, in addition to the potential determined by the gate voltage, it is also important to account for the effect of drain voltage on reaction rates.

In amperometric OECTs with an OMIEC gate, more complexities arise as there is no control over the potential of the gate or channel (only their potential difference). Hence, depending on the operation and processing history of the gate, the potentials on both the gate and channel can change. Furthermore, applying a gate voltage changes the relative reactivity of both the gate and channel.

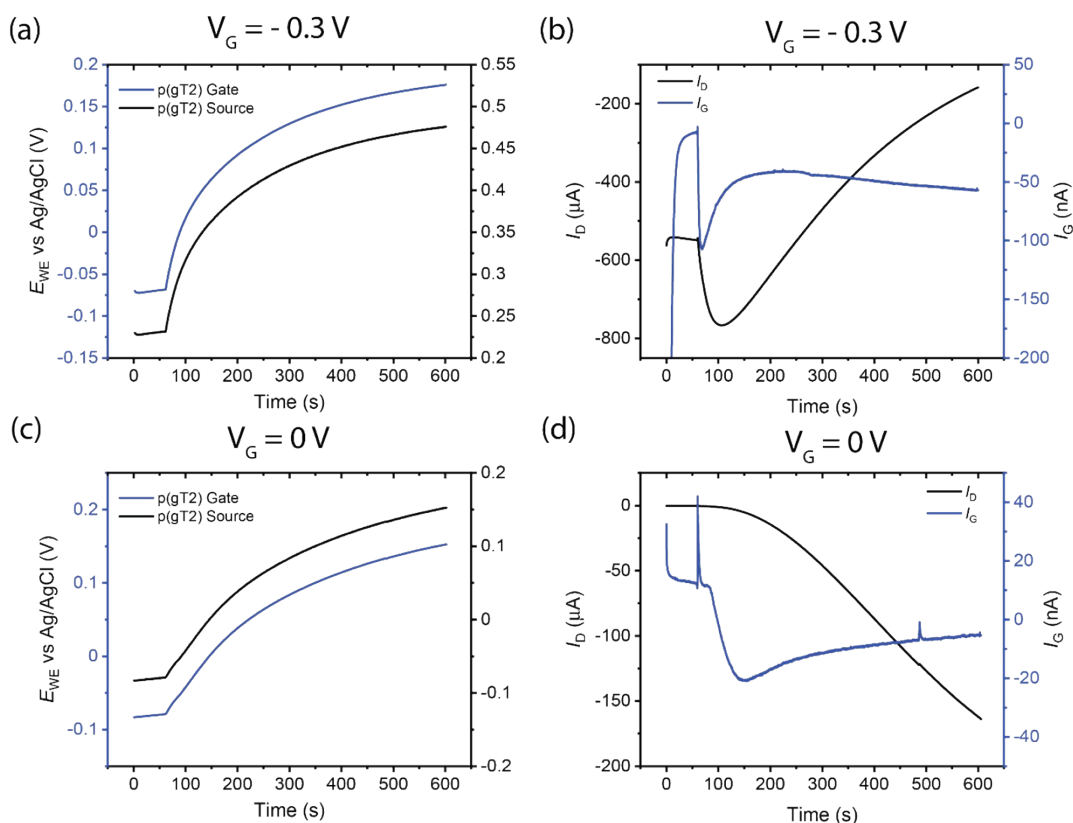


**SI Figure 2. Schematics of potential measurement of electrodes in different OEET architectures and their corresponding equivalent circuits. (a)** Schematic of amperometric OEET with Ag/AgCl gate showing addition of redox analyte to electrolyte while conducting potential measurements of the Ag/AgCl gate and source of the channel. **(b)** Equivalent circuit of amperometric OEET with Ag/AgCl gate showing flow of electrons as result of chemical redox reaction on the channel. **(c)** Schematic of amperometric OEET with OMIEC gate showing addition of redox analyte to electrolyte while conducting potential measurements of the OMIEC gate and source of the channel. **(d)** Equivalent circuit of amperometric OEET with Ag/AgCl gate showing

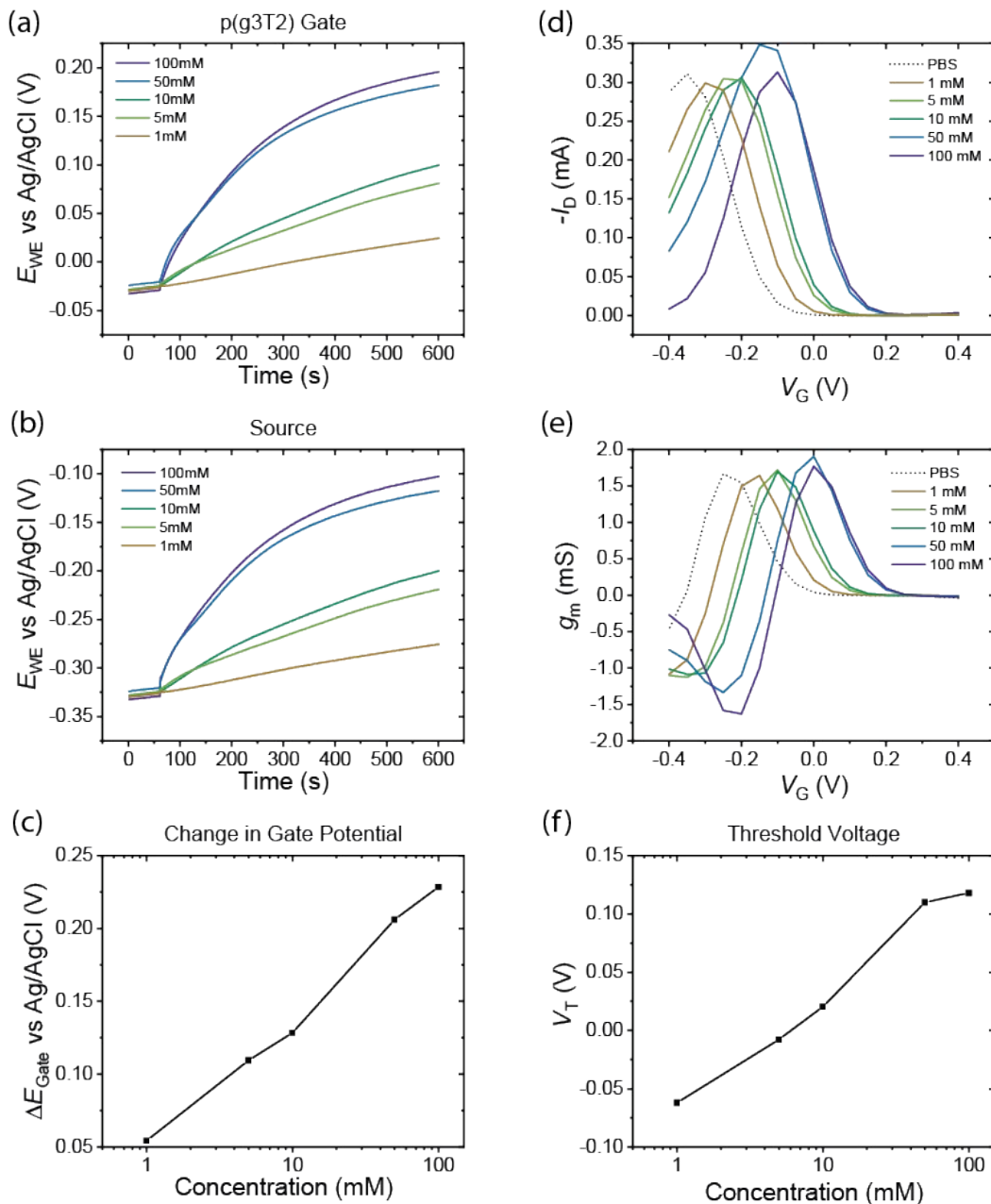
flow of electrons as result of chemical redox reaction on the channel and gate. **(e)** Schematic of RC and OECT where the RC anode is in electrical contact with the OECT's Ag/AgCl gate electrode and the RC cathode is in electrical contact with the source. Redox analyte is added to RC's electrolyte while conducting potential measurements on the RC's anode, cathode as well as the OECT's gate and source. **(f)** Sketch of equivalent circuit of RC-OECT showing the oxidation reaction primarily on the anode and the flow of electrons from the OECT to the RC.



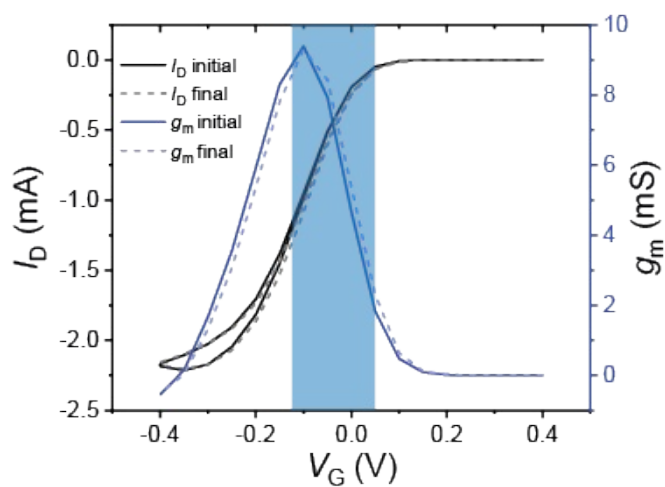
**SI Figure 3. Gate current of Amperometric OECT (with OMIEC gate) during a transfer curve measurement. Solid line: Pristine state in PBS. Dashed line: After addition of 33 mM  $\text{H}_2\text{O}_2$  to OECT electrolyte. Red arrow shows larger reaction currents at more positive gate voltages.**



**SI Figure 4. Operation of A-OECT (OMIEC gate) at different gate voltages and addition of 33 mM  $\text{H}_2\text{O}_2$ . (a)  $V_G = -0.3$  V. Plot of p(gT2) gate (blue) and source (black) potentials. (b)  $V_G = -0.3$  V. Plot of gate (blue) and drain (black) current. (c)  $V_G = 0$  V. Plot of p(gT2) gate (blue) and source (black) potentials. (d)  $V_G = 0$  V. Plot of gate (blue) and drain (black) current.**



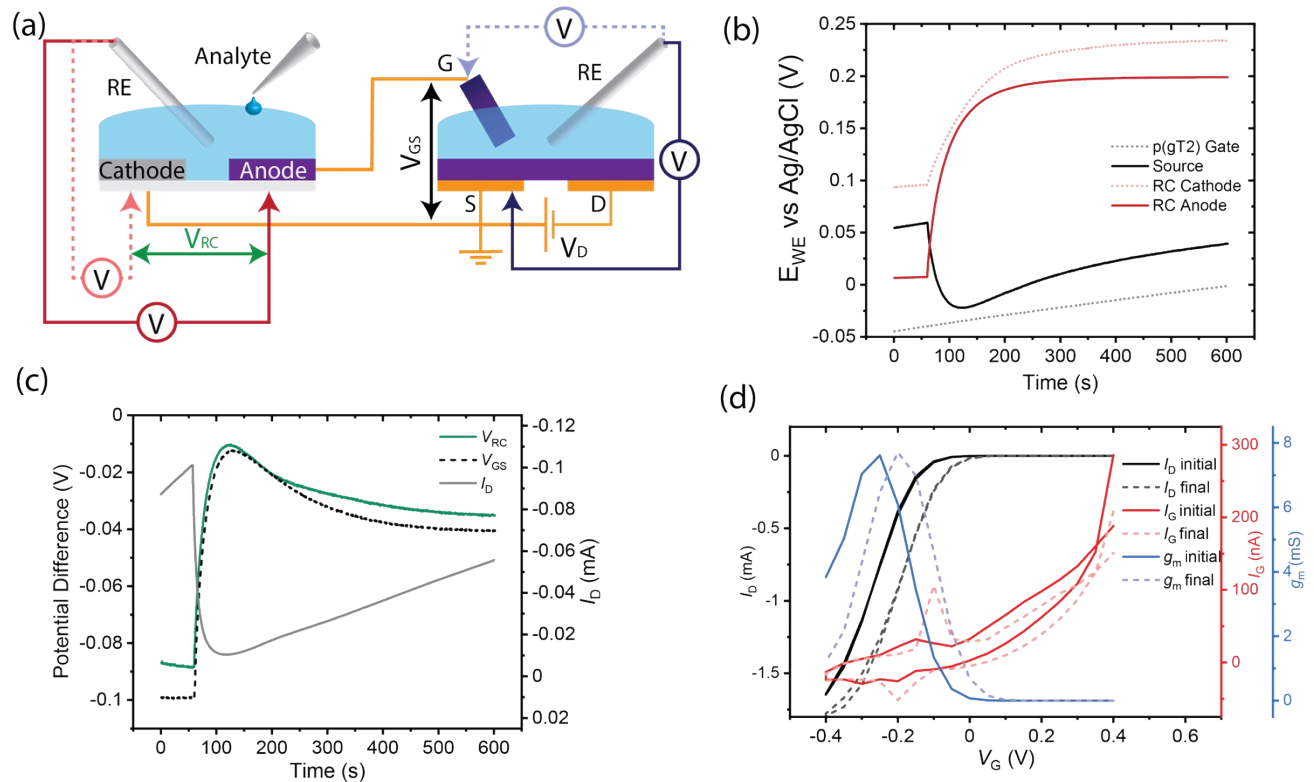
**SI Figure 5. Amperometric OECT with OMIEC gate: effect of different concentrations of  $\text{H}_2\text{O}_2$ .** (a) Measurement of potential on the p(g3T2) gate with  $V_G = +0.3 \text{ V}$ . Different concentrations of 100  $\mu\text{L}$   $\text{H}_2\text{O}_2$  are added to 200  $\mu\text{L}$  of PBS OECT electrolyte at 60s. (b) Concurrent measurement of potential on the source. (c) Plot of change in gate potential vs  $\text{H}_2\text{O}_2$  concentration. (d) Transfer curves of the OECT in its initial state (PBS electrolyte) and after addition of  $\text{H}_2\text{O}_2$  of various concentrations. (e) Corresponding transconductance of OECT in its initial state (PBS electrolyte) and after addition of  $\text{H}_2\text{O}_2$  of various concentrations. (f) Plot of OECT threshold voltage vs  $\text{H}_2\text{O}_2$  concentration.



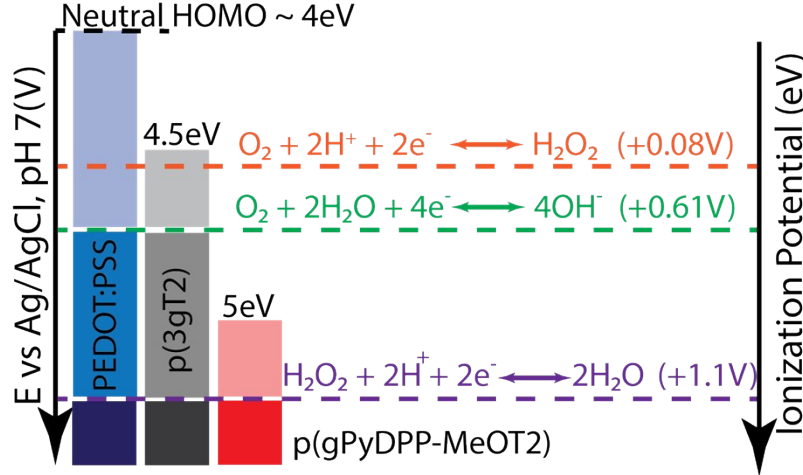
**SI Figure 6.** Transfer curve (black) and transconductance (blue) of the OEECT in its initial state (solid traces) and after addition of the redox analyte to the electrolyte (dashed). Blue rectangle indicate range of  $V_{RC}$ .

Stability of OEECT before and after RC-OECT operation allows the same OEECT to be utilized for multiple reactions by changing RCs.



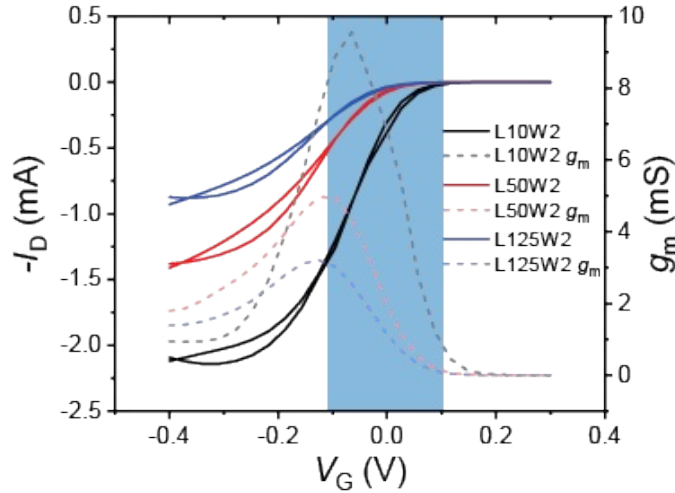


**SI Figure 7. Reaction Cell OEET with OMIEC gate electrode in OEET.** (a) Schematic of RC and OEET where the RC anode is in electrical contact with the OEET's OMIEC gate electrode and the RC cathode is in electrical contact with the source. Redox analyte is added to RC's electrolyte while conducting potential measurements on the RC's anode, cathode as well as the OEET's gate and source. (b) Plot of potentials of OMIEC gate electrode (grey dashed), OEET source (grey solid), RC anode (red solid) and RC cathode (red dashed). (c) Plot of potential differences across RC (green) and OEET's gate-source (black dashed) as well as the drain current (grey) and the calculated drain current (grey dashed). (d) Transfer curve (black), gate currents (red) and transconductance (blue) of the OEET in its initial state (solid traces) and after addition of the redox analyte to the electrolyte (dashed).



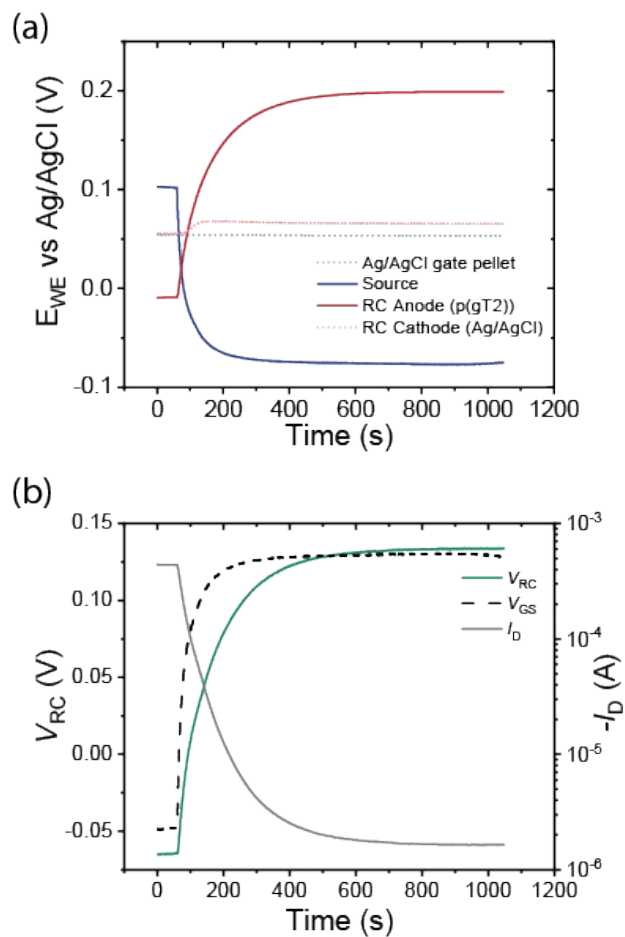
**SI Figure 8.** Schematic of the energy levels of the p-type polymers PEDOT:PSS (blue), p(3gT2) (black) and p(gPyDPP–MeOT2) (red) relative to ORR and HPRR. Lighter colors indicate that the polymers are charged (oxidized) due to ORR (ambient conditions).

To improve the magnitude of potential change of the anode, the anode's ionization potential (IP) should be low enough such that the driving force for electron transfer from the valence band to the analyte of interest is maximized. Yet, the polymer's IP should not be low such that it is too susceptible to oxidation by oxygen at ambient conditions (e.g. PEDOT:PSS). p(3gT2) has an IP that is a reasonable balance between these two extremes.

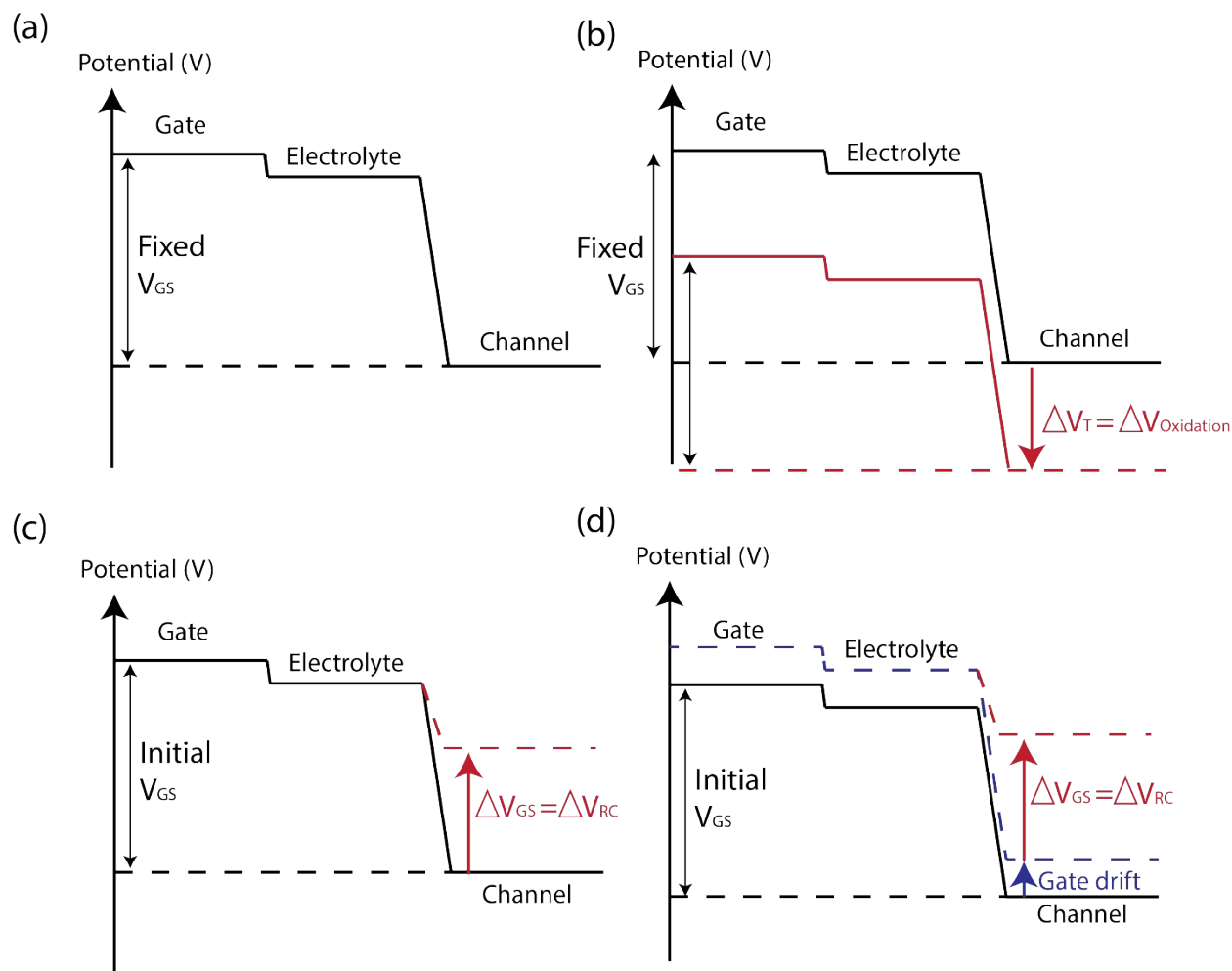


**SI Figure 9.** Transfer curves (dark solid lines) and transconductances (light dashed lines) of OEECTs  $W = 2000 \mu m$ ,  $L = 10 \mu m$  (black),  $50 \mu m$  (red),  $125 \mu m$  (blue),  $d = 120 nm$  operated at  $V_D = -0.1 V$ .

Increasing the W/L aspect ratio of the OEECT channel increases its transconductance and shifts the maximum transconductance to  $V_{GS}$  values closer to 0 V. Hence, the shortest channel OEECT ( $W = 2000 \mu m$ ,  $L = 10 \mu m$ ,  $d = 120 nm$ ) geometry was selected for this study.

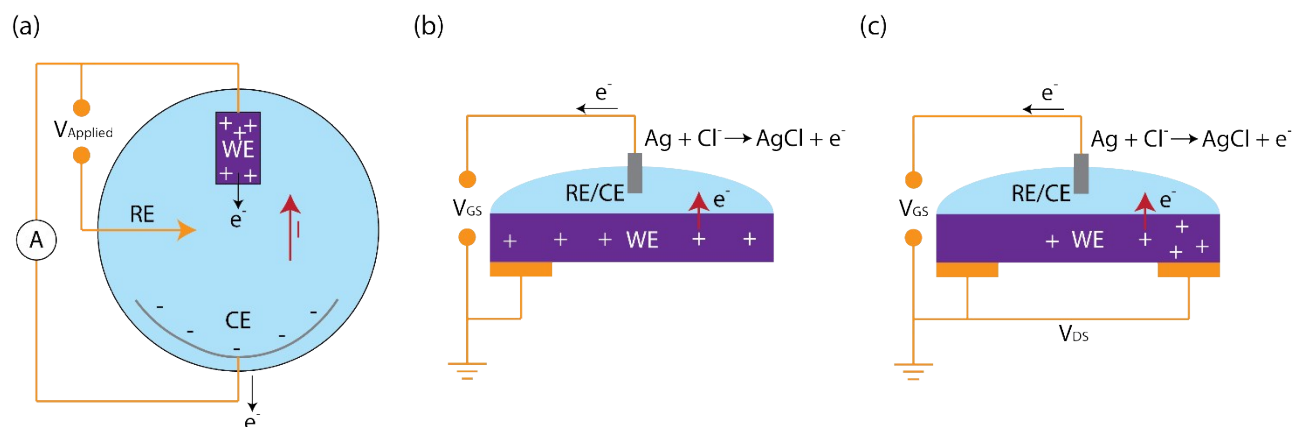


**SI Figure 10. Effect of changing RC cathode to Ag/AgCl pellet. (a)** Plot of potentials of Ag/AgCl gate electrode (grey dashed), OECT source (grey solid), RC p(g3T2) anode (red solid) and RC Ag/AgCl cathode (red dashed). **(b)** Plot of potential differences across RC (green) and OECT's gate-source (black dashed) as well as the drain current (grey).



**SI Figure 11. Illustration of potential profiles with the OECT from gate, to electrolyte and channel for different OECT chemical sensor architectures** (a) Amperometric OECT with Ag/AgCl gate. No potential changes are observed due to the fixed gate potential and gate voltage. (b) Amperometric OECT with OMIEC gate. Potentials throughout the OECT shift in concert due to oxidation of both gate and channel as well as the fixed gate voltage. (c) RC-OECT with Ag/AgCl gate. Potential drop occurs mainly on the channel which changes by the same amount as  $\Delta V_{RC}$ . (d) RC-OECT with OMIEC gate. Potential drop occurs mainly on the channel which changes by the same amount as  $\Delta V_{RC}$ . There is additional shift in potentials across the OECT due to drift in gate potential.

## Modelling of Ideal Amperometric Sensors



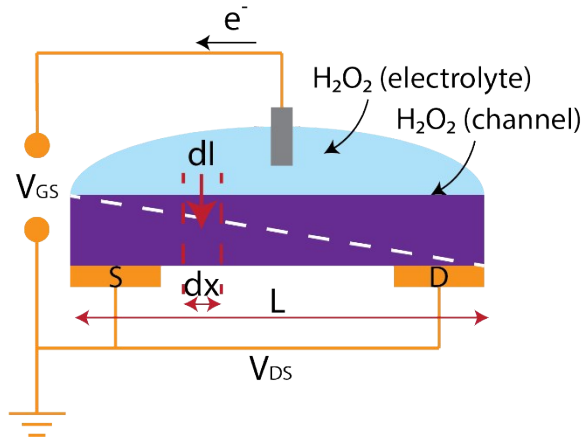
**SI Figure 12. Comparison of 3-electrode and 2-electrode amperometric sensors. (a)** 3-electrode setup **(b)** 2-electrode setup with the absence a counter electrode **(c)** 2-electrode setup where conductivity of the working electrode is measured (OECT)

In a regular amperometric sensor (**SI Figure 12 (a)**), a potential is applied between a reference electrode (RE) and a working electrode (WE) while ensuring that there is minimal current flow between these two electrodes. For example, a saturated Ag/AgCl reference consists of a saturated aqueous solution of  $Cl^-$  ions (e.g. KCl), Ag (s) and AgCl (s) such that the activities of the all three phases are constant, resulting in constant electrochemical potential of the reference electrode. Hence, the potential on the working electrode can be measured against a known value. In chronoamperometry measurements, the potential difference between the RE and WE is fixed by the potentiostat e.g. the initial open circuit potential. When  $H_2O_2$  is introduced to the electrolyte, the oxidation of p(g3T2) leads to the injection of holes into the film. The accumulation of holes on p(g3T2) would lead to shifts in its potential which is not allowed in CA. Hence, an external current must flow from the potentiostat into the WE to maintain a constant OCV vs. the reference. For the circuit to be complete, an additional counter electrode (CE) is required to collect this current. In this 3-electrode setup, the current (or charge) injected into the WE is solely due to the compensation of charges generated by HPRR at the specific potential applied. The reaction current dependence on applied potentials can be expressed by the Butler-Volmer model. For a fixed potential, the Cottrell equation can be used to relate the reaction current to concentration.

To progress to the OECT sensor, let's first look at a pseudo amperometric sensor, which unlike the 3-electrode setup, lacks a counter electrode. In this case, an Ag/AgCl pellet is used as a reference and a potential is applied between the pellet and the polymer. To catalyze the HPRR on the polymer, a positive potential difference is applied on the pellet with respect to the WE (e.g. +0.3 V), resulting in negative potentials on the WE. This leads to the reduction of hydrogen peroxide on the polymer and oxidation of Ag to AgCl on the pellet. Due to the absence of a counter electrode, current must flow through the reference electrode. Electrons from the oxidation of Ag flow from the pellet through the external circuit and replenish the holes generated on the polymer to maintain a constant potential difference between the pellet and polymer. The pellet here is not an ideal reference electrode as redox reactions of Ag are forced to occur which may lead to changes

in  $\text{Cl}^-$  concentrations in the electrolyte. In the limit where  $\text{Cl}^-$  concentration is constant, the current measured would be the absolute amount of charge generated by HPRR at the applied potential (e.g. -0.3V vs. Ag/AgCl).

In an OECT sensor, the measured source-drain current does not capture the absolute amount of charge but how the injected charges affect conductivity of the channel which adds an additional layer of complexity to the understanding of device operation. The channel is a variable resistor where the applied  $V_{GS}$  modulates the channel conductivity and this conductivity can be probed by applying a  $V_{DS}$  across the channel and measuring drain current ( $I_D$ ). Concurrently, as discussed above,  $V_G$  also controls the rate of HPRR. Unlike other field effect transistors where  $V_{GS} \gg V_{DS}$ , the fact that  $V_{DS}$  is on a similar magnitude as  $V_{GS}$  for an OECT results in further perturbation of the HPRR rate by  $V_{DS}$ . **SI Figure 13** summarizes the effect of asymmetric electric fields within the OECT.



**SI Figure 13. Illustration of approach to model faradaic reaction currents in an OECT.  $dI$  is the current injected into a slice of  $dx$  across the channel length.**

Boundary conditions: Potentials are fixed by externally applied voltages to drive redox reactions. Hence, the OECT is at non-equilibrium conditions. To approximate the change in source-drain current in the OECT channel, we can use a modified Butler-Volmer model:

The potential across the channel varies linearly, where  $x$  is the position from the source:

$$V_{CH}(x) = \frac{x}{L}V_D + V_G$$

For each infinitesimal slice ( $dx$ ) along the length of the channel, the infinitesimal reaction current ( $dI$ ) dependent on the potential across the length of the channel can be expressed according to the Butler-Volmer model. Here, we only consider HPRR and can neglect the oxidation reaction of  $\text{H}_2\text{O}_2$  as we are applying large positive gate potentials to drive HPRR on the OECT channel:

$$dI(x) = I_0 \left\{ \frac{[\text{H}_2\text{O}_2]_{\text{channel}}(t)}{[\text{H}_2\text{O}_2]_{\text{electrolyte}}} \exp \left( - \frac{\alpha F \eta(x)}{RT} \right) \right\}$$

$$\eta(x) = \frac{x}{L}V_D + V_G - E_0$$

Where  $I_0$  is the exchange current,  $\alpha$  is the transfer coefficient, and  $\eta$  is the overpotential ( $E_{\text{applied}} - E_0$ ). In this case,  $E_{\text{applied}} = V_{\text{CH}}$ , the potential on the channel. The exchange current is dependent on the surface area of the channel.  $k^0$  is the standard rate constant of the reaction:

$$I_0 = FWLk^0([H_2O_2]_{\text{electrolyte}})^{(1-\alpha)}$$

$$dI(x,t) = FWLk^0([H_2O_2]_{\text{electrolyte}})^{-\alpha} \left\{ [H_2O_2]_{\text{channel}}(t) \cdot \exp\left(-\frac{\alpha F \eta(x)}{RT}\right) \right\} dx$$

As the system is not in equilibrium, we need to account for the change in concentration of  $H_2O_2$  at the channel surface which will be depleted over time and needs to be replenished by diffusion from the bulk of the electrolyte (modified from Cottrell equation, where we assume interfacial reaction kinetics are more rapid than mass transfer i.e. the channel is a sink for  $H_2O_2$ ):

$$Flux, J_{H_2O_2\text{channel}}(0, t) = \frac{[H_2O_2]_{\text{electrolyte}}\sqrt{D}}{\sqrt{\pi t}}$$

### Charge accumulation (OMIEC gate): Current Transients

We first investigate the phenomena in an amperometric OECT with OMIEC gate. Experimental data in **Figure 3** and **SI Figure 4** show the shift in threshold voltage after addition of  $H_2O_2$  is indicative of charge accumulation on the channel. To model the time-dependent change in drain current, we assume:

1. Applied gate voltage is above the initial threshold voltage of the OECT, hence operating the OECT in the super-threshold regime. This is so that charge injected in the channel from the reaction results in the depletion of the valence band (accumulation of holes) and hence a change in charge density.
2. For simplicity, mobility is assumed to be independent of charge density. This may not hold true for all ranges of  $V_{GS}$  as  $g_m$  is not a constant with respect to  $V_G$ . In particular, mobility is limited at potentials near the oxidation onset of the p-type channel ( $V_T$ ).
3. No degradation of the polymer channel nor side reactions. This may not be the case at extreme potentials that result in permanent chemical changes in the polymer molecular structure and hence its electrochemical properties.
4. The bulk concentration of analyte in the electrolyte remains unperturbed.
5. All the charge injected ( $\Delta Q$ ) into the channel is due to reaction of the oxidant on the channel.

This leads to its change in conductivity (due to changes in density of charge carriers i.e. changing the volumetric capacitance of the channel). We then sum up the total amount of  $H_2O_2$  entering the channel over the whole course of the experiment. The change in source-drain current (from Ohm's Law) would be:

$$\Delta I_{CH} = V_D \cdot \frac{Wd}{L} \cdot \mu \cdot \Delta Q_{cumulative}$$

To get the instantaneous concentration of  $H_2O_2$  at the surface of the channel, we integrate flux over time.

$$Instantaneous [H_2O_2]_{channel}(t) = \frac{2[H_2O_2]_{electrolyte}\sqrt{Dt}}{\sqrt{\pi}}$$

$$\Delta Q_{cumulative} = \int_0^t \Delta Q_{instantaneous} dt = FWLk^0([H_2O_2]_{electrolyte})^{(1-\alpha)} \int_0^t \int_0^L \left\{ \frac{2\sqrt{Dt}}{\sqrt{\pi}} \exp\left(-\frac{\alpha F\left(\frac{x}{L}V_D + V_G - E_0\right)}{RT}\right) \right\} dx dt$$

Hence,

$$\Delta I_{CH}(t) = V_D \cdot W^2 d \cdot \mu \cdot F k^0 ([H_2O_2]_{electrolyte})^{(1-\alpha)} \int_0^t \int_0^L \left\{ \frac{2\sqrt{Dt}}{\sqrt{\pi}} \cdot \exp\left(-\frac{\alpha F\left(\frac{x}{L}V_D + V_G - E_0\right)}{RT}\right) \right\} dx dt$$

Which simplifies to:



$$\Delta I_{CH}(t) = W^2 dL \cdot \mu \cdot F k^0 ([H_2O_2]_{electrolyte})^{(1-\alpha)} \cdot \frac{4\sqrt{D}t^{3/2}}{3\sqrt{\pi}} \cdot \left\{ \frac{1}{\beta} \exp[-\beta(V_G - E_0)] \cdot \left[ 1 - \exp\left(-\frac{\beta V_D}{L}\right) \right] \right\}$$

Where:  $\beta = \frac{\alpha F}{RT}$

Let  $\gamma = F k^0 ([H_2O_2]_{electrolyte})^{(1-\alpha)} \frac{\sqrt{D}}{\sqrt{\pi}} \left\{ \frac{1}{\beta} \exp[-\beta(V_G - E_0)] \cdot \left[ 1 - \exp\left(-\frac{\beta V_D}{L}\right) \right] \right\}$

So  $\Delta I_{CH}(t) = W^2 dL \cdot \mu \cdot \frac{4t^{3/2}}{3} \cdot \gamma$

Total charge injected into the channel must equal the gate.

$$\Delta Q_{cumulative, gate} = \Delta Q_{cumulative, channel}$$

$$\Delta I_{Gate} = \frac{d(\Delta Q_{cumulative})}{dt} = FWL^2 k^0 ([H_2O_2]_{electrolyte})^{(1-\alpha)} \cdot \frac{2\sqrt{Dt}}{\sqrt{\pi}} \cdot \frac{1}{V_D} \left\{ \frac{1}{\beta} \exp[-\beta(V_G - E_0)] \cdot \left[ 1 - \exp\left(-\frac{\beta V_D}{L}\right) \right] \right\}$$

$$\Delta I_{Gate} = \frac{d(\Delta Q_{cumulative})}{dt} = WL^2 \cdot \frac{2\sqrt{t}}{V_D} \cdot \gamma$$

This analysis shows that the drain current of the amperometric OECT (with OMIEC gate) does not converge to a steady state on reasonable time scales under the above assumptions and boundary conditions. This is indeed observed in **SI Figure 3 (d)** where drain current increases steadily with a time dependence  $\sim t^{3/2}$  even when potential changes on the gate and channel begin to plateau off (**SI Figure 3 (c)**).

This model only holds for the above assumptions. When the OECT is operated at negative gate voltages (**SI Figure 3 (a-b)**), addition of an oxidizing agent results in over oxidation of the channel, resulting in a drop in conductivity of the channel. When the OECT is operated in the subthreshold regime as shown in **Figure 3 (c)**, there is no charge accumulation on the channel, and the OECT behaves similar to the case with a non-polarizable gate (see next section).

### Amperometric operation of OECT (Ag/AgCl gate)

In the other limit, the charges generated by the reduction of  $H_2O_2$  do not lead to accumulation of charges within the channel, so the charge density in the channel is only modified by the flux of  $H_2O_2$ . Whatever charges that enter the channel get swept into the current flowing through the conductor.

$$\Delta I_{CH} = V_D \cdot \frac{Wd}{L} \cdot \mu \cdot \Delta Q_{Flux}$$

$$\text{Let } \gamma = Fk^0([H_2O_2]_{electrolyte})^{(1-\alpha)} \frac{\sqrt{D}}{\sqrt{\pi}} \left\{ \frac{1}{\beta} \exp[-\beta(V_G - E_0)] \cdot \left[ 1 - \exp\left(-\frac{\beta V_D}{L}\right) \right] \right\}$$

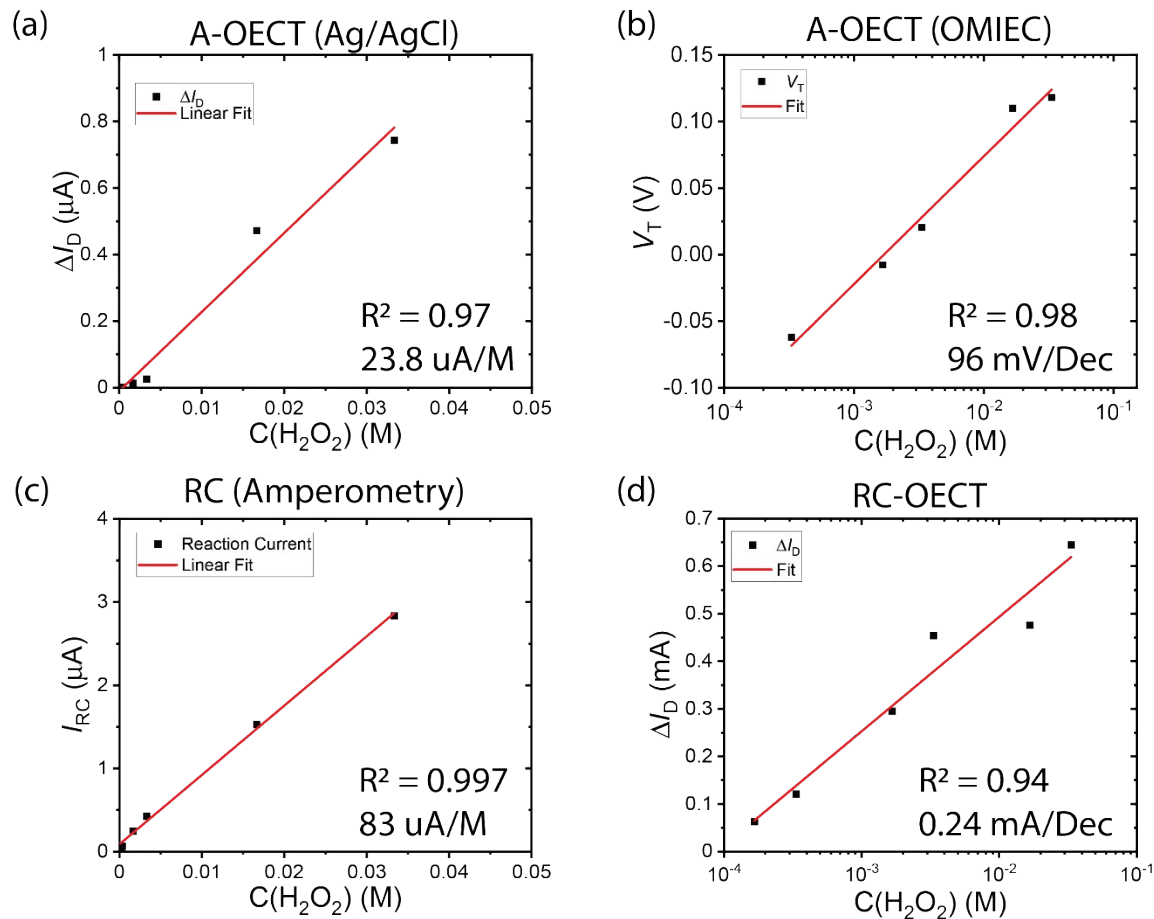
$$\Delta I_{CH} = V_D \cdot \frac{Wd}{L} \cdot \mu \cdot FWLk^0([H_2O_2]_{electrolyte})^{(1-\alpha)} \frac{2\sqrt{D}}{\sqrt{\pi t}} \int_0^L \left\{ \exp\left(-\frac{\alpha F \left(\frac{x}{L} V_D + V_G - E_0\right)}{RT}\right) \right\} dx$$

$$\Delta I_{CH}(t) = W^2 dL \cdot \mu \cdot Fk^0([H_2O_2]_{electrolyte})^{(1-\alpha)} \cdot \frac{2\sqrt{D}}{\sqrt{\pi t}} \cdot \left\{ \frac{1}{\beta} \exp[-\beta(V_G - E_0)] \cdot \left[ 1 - \exp\left(-\frac{\beta V_D}{L}\right) \right] \right\}$$

$$\Delta I_{CH}(t) = W^2 dL \cdot \mu \cdot 2t^{-1/2} \cdot \gamma$$

$$\Delta I_{Gate} = \Delta Q_{instantaneous} = FWL^2 k^0([H_2O_2]_{electrolyte})^{(1-\alpha)} \cdot \frac{2\sqrt{Dt}}{\sqrt{\pi}} \cdot \frac{1}{V_D} \left\{ \frac{1}{\beta} \exp[-\beta(V_G - E_0)] \cdot \left[ 1 - \exp\left(-\frac{\beta V_D}{L}\right) \right] \right\}$$

Without permanent charge accumulation on the channel, the time-dependence of current in an amperometric OECT scales in a similar way to that of the Cottrell equation of an amperometric measurement conducted in a three-electrode electrochemical cell.



**SI Figure 14.** Comparison of sensing performance for A-OECTs and RC-OECT. Sensitivity is extracted from fits. (a) A-OECT (Ag/AgCl gate) drain current modulation measured at  $V_G = +0.3$  V,  $V_D = -0.1$  V, plotted on a linear scale. (b) Threshold voltage of A-OECT (OMIEC gate) measured at  $V_D = -0.1$  V, plotted on a log-linear scale. (c) RC reaction current vs  $H_2O_2$  concentration measured in the RC using chronoamperometry at 0 V vs Ag/AgCl, plotted on linear scale. (d) Magnitude of change in RC-OECT drain current vs  $H_2O_2$  concentration after amplification,  $V_D = -0.1$  V, plotted on log-linear scale.